


1 **Steady-state solutions for subsurface chlorophyll maximum in**
2 **stratified water columns with a bell-shape vertical profile of**
3 **chlorophyll**

4 X. Gong, J. Shi, H. W. Gao, X. H. Yao

5 Key Laboratory of Marine Environment and Ecology (Ministry of Education of
6 China), Ocean University of China, Qingdao 266100, China

7 Correspondence to: H. W. Gao (hwgao@ouc.edu.cn)

8 **Abstract:**

9 A bell-shape vertical profile of chlorophyll a (Chl a) concentration, conventionally
10 referred to as Subsurface Chlorophyll Maximum (SCM) phenomenon, has frequently
11 been observed in stratified oceans and lakes. This profile is assumed to be a general
12 Gaussian distribution in this study. By substituting the general Gaussian function into
13 ecosystem dynamical equations, the steady-state solutions for SCM characteristics
14 (i.e., SCM layer depth, thickness, and intensity) in various scenarios are derived.
15 These solutions indicate that: 1) The maximum concentration of Chl a occurs at or
16 below the depth of maximum growth rates of phytoplankton located at the transition
17 from nutrient limitation to light limitation, and the depth of SCM layer deepens
18 logarithmically with an increase in surface light intensity; 2) The shape of SCM layer
19 (thickness and intensity) is mainly affected by nutrient supply, but independent of
20 surface light intensity; 3) The intensity of SCM layer is proportional to the diffusive
21 flux of nutrients from below, getting stronger as a result of this layer being shrunk by
22 a higher light attenuation coefficient or a larger sinking velocity of phytoplankton. In
23 addition, the limitation and potential application of the analytical solutions w also
24 presented.

25 **1 Introduction**

26 Vertical profiles of chlorophyll a (Chl a) concentration in lakes, coastal seas and open
27 oceans are highly variable. However, a bell-shape vertical profile of Chl a,
28 conventionally referred to as Subsurface Chlorophyll Maximum (SCM) phenomenon,
29 has been frequently observed in stratified water columns, e.g., it occurred through the
30 whole year in tropical and subtropical oceans while it existed only during summer in
31 temperate and high latitude oceanic zones. The subsurface biomass maxima (SBMs)
32 are also common in stratified water columns. The chlorophyll-to-biomass ratio
33 generally increases with depth in the euphotic zone. Thus, SCMs may not necessarily
34 represent SBMs (Cullen, 1982; Fennel and Boss, 2003) and are usually deeper than
35 SBMs (Fennel and Boss, 2003; Hodges and Rudnick, 2004). However, both the
36 subsurface maxima in chlorophyll and biomass are usually formed in certain regions
37 of the water column where two opposing resource (light and nutrient) gradients
38 combined with vertically heterogeneous turbulent mixing is amenable for survival of
39 phytoplankton. Thus, SCMs are approximately equal to SBMs in many studies
40 (Klausmeier and Litchman, 2001; Sharples et al., 2001; Huisman et al., 2006; Raybov
41 et al., 2010). Fennel and Boss (2003) reported that the photoacclimation of
42 phytoplankton can be another important reason for forming a SCM in oligotrophic
43 waters.

44 The SCM phenomenon can be characterized by the thickness, depth, and intensity of
45 SCM layer (SCML) (Beckmann and Hense, 2007). On-site observations (Platt et al.,
46 1988; Sharples et al., 2001; Deksheniaks et al., 2001; Mellard et al., 2011) showed
47 that the SCML occurred relatively shallow (1-50 m) and was thin (several centimeters
48 to a few meters) in lakes and coastal seas, but the concentration of Chl a was high
49 (1-100 mg/m³). In open oceans, the SCML was deeper (80-130 m) and thicker (tens
50 of meters) while the concentration of Chl a was relatively low (<1 mg/m³) (Anderson,
51 1969; Platt et al., 1988).

52 SCM has attracted much attention because of the significant contribution of SCML to
53 the total biomass and primary production in the whole water column (Cullen and
54 Eppley, 1981; Weston et al., 2005; Siswanto et al., 2005; Hanson et al., 2007;
55 Sullivan et al., 2010). Pérez et al. (2006) showed that 65-75% of the total Chl a in a
56 water column of the Atlantic subtropical gyres was presented in SCML and the layer

57 thickness was approximately 50 m. Weston et al. (2005) reported that the SCML
58 accounted for 58% of the water column primary production in the central North Sea,
59 although the layer thickness was less than 5 m. Sullivan et al. (2010) found that the
60 fraction of Chl a in the SCML (thickness <3 m) out of the total water column ranged
61 from 33% to 47% in the Monterey Bay.

62 Many numerical studies have been conducted to link the thickness, depth and
63 intensity of the SCML to various environmental parameters (Jamart et al., 1979;
64 Varela et al., 1994; Klausmeier and Litchman, 2001; Hodges and Rudnick, 2004;
65 Huisman et al., 2006; Beckmann and Hense, 2007). The thickness of the SCML
66 mainly depends on the degree of vertical mixing in lakes (Klausmeier and Litchman,
67 2001). In oligotrophic oceans, light attenuation coefficient is the key factor in
68 determining the SCML depth (Varela et al., 1994; Hodges and Rudnick, 2004;
69 Beckmann and Hense, 2007) and the intensity of the SCML depends strongly on
70 sinking velocity of phytoplankton and vertical diffusivity rather than growth rate of
71 phytoplankton (Hodges and Rudnick, 2004; Beckmann and Hense, 2007). However,
72 the thickness, depth and intensity of SCML are very sensitive to variations of
73 environmental parameters. Therefore, the relationships obtained from a particular
74 case may not be applicable for other cases. To understand the general relationships
75 between SCM phenomenon and environmental parameters, the analytical solution for
76 dynamic ecosystem equations is needed.

77 The algae game theoretical model, pioneered by Klausmeier and Litchmann (2001),
78 was perhaps the first one to derive the depth and intensity of SCML, although the
79 SCML is assumed to be infinitely thin. They adopted a delta function to approximate
80 the phytoplankton distribution in this thin layer. Yoshiyama et al. (2009) used this
81 model to examine more than one species competing for limiting nutrients and light
82 below the surface mixed layer. Mellard et al. (2011) included stratification into this
83 model. However, the SCML was still confined to an infinitely thin layer. In fact,
84 many observations showed that the thickness of SCML can reach as high as 100 m in
85 oceans (Platt et al., 1988). For those cases, the assumption of an infinite thickness of
86 SCML is contradictory to the observations.

87 In this study, we assume that the vertical profile of Chl a can be approximately treated
88 as a general Gaussian function, instead of a delta function. This parameterizing
89 approach was proposed firstly by Lewis et al. (1983), and has been widely used to fit

90 vertical profiles of Chl a (Platt et al., 1988; Weston et al., 2005; Ardyna et al., 2013).
 91 By incorporating the general Gaussian function into the ecosystem dynamical
 92 equations, we derive the steady-state solutions for the thickness, depth, and intensity
 93 of SCML in various scenarios and examine their dependence on environmental
 94 parameters, such as light attenuation coefficient, vertical diffusivity, sinking velocity
 95 of phytoplankton.

96 2 Methods

97 2.1 Models

98 The SCML occurs below the surface mixed layer, where the light attenuated from
 99 above and nutrients supplied from the deep water match best for phytoplankton
 100 growth (Fig. 1). The partial differential equations for phytoplankton and nutrients
 101 dynamics in which light and nutrients are two major limited factors (Eqs. 1, 2) (Riley
 102 et al., 1949; Lewis et al., 1986; Gabric and Parslow, 1989; Huisman et al., 2006;
 103 Liccardo et al., 2013) were adopted in this study. Moreover, the photoacclimation of
 104 phytoplankton was not considered here and the Chl a distribution is supposed to
 105 represent the distribution of phytoplankton biomass. This is a significant
 106 simplification. In fact, phytoplankton increases inter-cellular pigment concentration
 107 when light level decreases (Fennel and Boss, 2003).

$$108 \quad \frac{\partial P}{\partial t} = \mu_m \min(f(I), g(N))P - \varepsilon P - w \frac{\partial P}{\partial z} + \frac{\partial}{\partial z} \left(K_v \frac{\partial P}{\partial z} \right), \quad (1)$$

$$109 \quad \frac{\partial N}{\partial t} = -\mu_m \min(f(I), g(N))P + \alpha \varepsilon P + \frac{\partial}{\partial z} \left(K_v \frac{\partial N}{\partial z} \right), \quad (2)$$

110 where P denotes the Chl a concentration, N is the limiting nutrient concentration.
 111 Usually, the unit of Chl a concentration is mg m^{-3} , the concentrations of
 112 phytoplankton and the limiting nutrients are in unit of mmol N m^{-3} . A ratio of 1.59 g
 113 chlorophyll per mol nitrogen (Cloern et al., 1995; Oschlies, 2001) is thereby used for
 114 unit conversion. μ_m is the maximum growth rate of phytoplankton, ε is the loss
 115 rate of phytoplankton (including respiration, mortality, zooplankton grazing), α is
 116 the recycling rate of dead phytoplankton ($0 \leq \alpha \leq 1$). w is the sinking velocity of
 117 phytoplankton, which is non-negative in the chosen coordinate system and assumed
 118 to be constant with depths. K_v is the vertical turbulent diffusivity and it is much

119 larger within the surface mixed layer than that beneath. Here, K_v depends on depth
 120 in the following way (Hodges and Rudnick, 2004; Mellard et al., 2011):

$$121 \quad K_v = \begin{cases} K_{v1} & 0 < z < z_s, \\ K_{v2} & z_s < z < z_b, \end{cases} \quad (3)$$

122 where z_s is the depth of surface mixed layer, z_b is the bottom of water column or the
 123 location where the Chl *a* concentration reduces to nearly zero below the euphotic
 124 zone. We assume K_{v1} , K_{v2} are constant and K_{v1} is large enough to homogenize the Chl
 125 *a* and nutrient concentrations in the surface mixed layer.

126 A gradual transition from the surface mixed layer to the deep one written in terms of a
 127 generalized Fermi function is adopted (Ryabov et al., 2010), that is, $K_v(z) = K_{v2} +$
 128 $\frac{K_{v1}-K_{v2}}{1+e^{(z-z_s)/l}}$, where parameter l characterizes the width of the transition layer. In our
 129 study, we assumed this transition layer is finitely thin.

130 The growth limited function $\min(f(I), g(N))$ for light I and nutrients N is:

$$131 \quad \min(f(I), g(N)) = \min\left(\frac{I(z)}{K_I + I(z)}, \frac{N(z)}{K_N + N(z)}\right), \quad (4)$$

132 where K_I and K_N denote the half-saturation constants of light and nutrients,
 133 respectively. The net growth rate, $\mu_m \min(f(I), g(N)) - \varepsilon$, is positive only if both the
 134 light limiting term $\mu_m f(I)$ and nutrient limiting term $\mu_m g(N)$ are larger than the
 135 loss rate ε .

136 Light intensity is assumed to decrease exponentially with depth according to
 137 Lambert-Beer's law, i.e.,

$$138 \quad I(z) = I_0 \exp(-K_d z), \quad (5)$$

139 where I_0 is the surface light intensity and K_d is the light attenuation coefficient (Morel,
 140 1988). Assuming a constant K_d , we ignore the effects of the self-shading and the
 141 dissolved and particulate material on the attenuation coefficient.

142 The zero-flux boundary conditions for the phytoplankton at the surface and bottom of
 143 the water column are used. Furthermore, we assume a zero-flux boundary condition
 144 for nutrients at the surface, while nutrients are replenished from below. That is,



145

$$\begin{cases} K_{v1} \frac{\partial P}{\partial z} - wP = 0, & K_{v1} \frac{\partial N}{\partial z} = 0, & \text{at } z = 0, \\ K_{v2} \frac{\partial P}{\partial z} - wP = 0, & K_{v2} \frac{\partial N}{\partial z} = K_{v2} \frac{\partial N}{\partial z} \Big|_{z=z_b}, & \text{at } z = z_b. \end{cases} \quad (6)$$

146

147

148

149

In addition, Lewis et al. (1983) first proposed a general Gaussian distribution function (Eq. 7) to model the nonlinear feature of observed vertical Chl a profiles. In this study, this function is adopted to represent the bell-shape vertical distribution of Chl a (Fig. 1).

150

$$P(z) = P_{\max} e^{-\frac{(z-z_m)^2}{2\sigma^2}} \quad 0 \leq z \leq z_b, \quad (7)$$

151

152

153

154

155

where $P(z)$ is Chl a concentration as a function of depth z , and $P_{\max} = \frac{h}{\sigma\sqrt{2\pi}}$. The three Gaussian parameters (h , z_m , σ) can vary to characterize the SCM phenomenon. Thus h is the vertical integrated Chl a over the entire water column, z_m is the depth of the maximum Chl a (the peak of the bell-shape), and σ is the standard deviation of Gaussian function, which controls the width of the SCML.

156

2.2 Three SCM characteristics

157

158

159

160

161

162

163

164

165

166

167

168

169

170

171

172

The thickness of SCML can characterize the vertical extent of Chl a distribution below the surface mixed layer. It is still debatable how to best define the thickness of SCML. One easy definition is to use the width between two locations below and above the Chl a peak, where Chl a is a certain fraction (e.g. 50%, $100(e^{-1/2})\%$) of the maximum Chl a (Platt et al., 1988; Pérez et al., 2006). Some studies bounded the layer by sharp vertical gradients in Chl a above and below the peak (Prairie et al., 2011). Others defined the upper and lower boundary of SCML by ad hoc choices. Pedrós-Alió et al. (1999) proposed the SCML from the depth of the surface mixed layer to the lower maximum gradient in the slope of the Chl a profile. Hanson et al. (2007) defined that the upper boundary of the SCML was the minimum gradient criterion of $0.02 \text{ mg Chl a m}^{-1}$ and the lower was the base of the euphotic zone. Beckmann and Hense (2007) proposed to define the boundaries of SCML by the existence of two community compensation depths in the water column, which were located at the depths of two maximum phytoplankton gradients in phytoplankton biomass.

Building on the study by Beckmann and Hense (2007), the locations of the maximum

173 phytoplankton gradients are defined as the boundaries of SCML in this study. That is,

174
$$\left. \frac{d^2 P}{dz^2} \right|_{z=z_u, z_l} = 0, \quad (8)$$

175 where z_u and z_l are the upper and lower boundary of SCML, respectively.

176 By substituting Eq. (7) into this equality, we obtain $z_u = z_m - \sigma$, $z_l = z_m + \sigma$. Thus,
177 the thickness of SCML can thereby be expressed as 2σ .

178 From Eq. (8) and the steady state of Eq. (1), one gets the following equality at the
179 boundaries of SCML:

180
$$\left(\mu_m \min(f(I), g(N))P - \varepsilon P - w \frac{dP}{dz} \right) \Big|_{z=z_u, z_l} = 0. \quad (9)$$

181 That is, the boundary of SCML is located at the depth where there is the balance
182 between phytoplankton growth and all losses (including the divergence of the sinking
183 flux $w \frac{dP}{dz}$ and the loss ε due to mortality, respiration, and grazing), named the
184 community compensation depth (Ono et al., 2001). Thus, this definition reflects the
185 physical-biological ecosystem dynamics associated with SCML.

186 As described in Eq. (7), the depth of the SCML is defined as z_m , that is, the location
187 of the point-wise maximum value of Chl a.

188 The third quantity, i.e. the intensity of SCML, refers to the maximum value of Chl a
189 (P_{\max} in Eq. 7) in the water column.

190 *2.3 Approach used in this study*


191 Previous numerical studies (Huisman et al., 2006; Ryabov et al., 2010) showed that
192 the ecosystem dynamical model (Eqs. 1 and 2) can approximately reproduce the
193 bell-shape feature of the vertical Chl a profile (Fig. 1). We substitute the general
194 Gaussian function of the vertical Chl a profile (Eq. 7) into Eqs. (1) and (2) to derive
195 explicit relationships between three characteristics of SCM and the environmental
196 parameters.


197 Firstly, by substituting the general Gaussian function of $P(z)$ with the steady-state
198 version of Eq. (1), we obtain that below the surface mixed layer the net growth rate of
199 phytoplankton can be expressed as follows


200
$$\mu_m \min(f(I), g(N)) - \varepsilon = -\frac{K_{v2}}{\sigma^4} \left(z - z_m + \frac{w\sigma^2}{2K_{v2}} \right)^2 + \frac{w^2}{4K_{v2}} + \frac{K_{v2}}{\sigma^2}. \quad (10)$$

201 Letting $\mu_m \min(f(I), g(N)) - \varepsilon = 0$, we get the two compensation depths, z_{c1} , z_{c2} , by
 202 solving Eq. (10):

203
$$z_{c1} = z_m - \frac{w\sigma^2}{2K_{v2}} - \sqrt{\left(\frac{w\sigma^2}{2K_{v2}} \right)^2 + \sigma^2}, \quad z_{c2} = z_m - \frac{w\sigma^2}{2K_{v2}} + \sqrt{\left(\frac{w\sigma^2}{2K_{v2}} \right)^2 + \sigma^2}. \quad (11)$$

204  Clearly, the inequality $\mu_m \min(f(I), g(N)) - \varepsilon > 0$ is satisfied in the interval (z_{c1}, z_{c2}) .
 205 This indicates that the subsurface net production occurs only between the two
 206 compensation depths where the growth rate $\mu_m \min(f(I), g(N))$ equals the loss rate
 207 ε . Beckmann and Hense (2007) found similar results by numerical modeling and
 208 emphasized the often overlooked fact that an SCML has to have two compensation
 209 depths.

210 From Eq. (11), we obtain $z_{c1} \leq z_m - \sigma$ and $z_m \leq z_{c2} \leq z_m + \sigma$ (Fig. 1). Especially,
 211 $z_{c1} = z_m - \sigma$, and $z_{c2} = z_m + \sigma$ when the sinking velocity of phytoplankton w is too
 212 small to be  considered. This result is identical to that of Beckmann and Hense (2007)
 213 for neglecting sinking velocity of phytoplankton.

214 Hence, according to the property of quadratic function, there exists a depth z_0  within
 215 the two compensation depths,

216
$$z_0 = z_m - \frac{w\sigma^2}{2K_{v2}}, \quad (12)$$

217 such that the net growth rate of phytoplankton is at its maximum, i.e.,

218
$$\max(\mu_m \min(f(I), g(N)) - \varepsilon) \Big|_{z_0} = \frac{K_{v2}}{\sigma^2} + \frac{w^2}{4K_{v2}}. \quad (13)$$

219 In other words, the maximum in net growth rates of phytoplankton occurs at the
 220 depth of z_0 .

221 We define $T = \sigma^2 / K_{v2}$ as the characteristic vertical mixing time scale in the SCML of
 222 thickness σ (Bowdon, 1985; Gabric and Parslow, 1989). Let the length scale be
 223 $L = 2K_{v2} / w$, which determines the scale height of the phytoplankton distribution
 224 (Ghosal and Mandre, 2003). Thus, the right hand terms of Eq. (13) can be rewritten

225 as $1/T+w/(2L)$. In other words, the maximum net growth rate of phytoplankton,
 226 $\max(\mu_m \min(f(I), g(N)) - \varepsilon)$, is determined by the vertical mixing time scale (T) and
 227 the time taken by a phytoplankton sinking (w) through lengths ($2L$).

228 Equation (12) also shows that $z_m \geq z_0$, that is, the depth of SCML lies at or below
 229 the depth for phytoplankton having the maximum growth rate. Observations in the
 230 Southern California Bight have supported this (Cullen and Eppley, 1981).
 231 Particularly, $z_m = z_0$ approximately holds when either the sinking velocity (w) or
 232 Gaussian parameter σ is very small. For non-sinking phytoplankton, i.e., $w \rightarrow 0$,
 233 numerical modeling can support this equality (Beckmann and Hense, 2007). When
 234 parameter σ is assumed to be infinitely thin, the equality is obviously correct, which
 235 has been used to solve for the equilibrium depth and intensity of an infinitely thin
 236 layer (Klausmeier and Litchman, 2001; Yoshiyama et al., 2009; Mellard et al., 2011).

237 In this special case ($z_m = z_0$), some studies found that the depth of SCML is at the
 238 location of equal limitation by nutrients and light (Klausmeier and Litchman, 2001;
 239 Yoshiyama et al., 2009; Mellard et al., 2011). In this study, we further infer that when
 240 $z_m > z_0$, the depth of SCML is located at where phytoplankton growth is limited by
 241 light (Appendix A).

242 According to Eqs. (12) and (A2), the growth of phytoplankton is light-limited at and
 243 below the depth of SCML. Therefore, for $z = z_m$ and $z = z_m + \sigma$, the net growth rate
 244 of phytoplankton (Eq. 10) can be expressed as following, respectively:

$$245 \quad \mu_m f(I)|_{z=z_m} - \varepsilon = K_{v2} / \sigma^2 \quad (14)$$

$$246 \quad \mu_m f(I)|_{z=z_m+\sigma} - \varepsilon = -w / \sigma \quad (15)$$

247 At the depth of z_m , the net growth rate of phytoplankton (Eq. 14) is determined by
 248 the vertical mixing time, T , while the time taken by phytoplankton sinking through
 249 half-length of SCML, w/σ , controls the net growth rate of phytoplankton (Eq. 15) at
 250 the lower boundary of SCML ($z_m + \sigma$).

251 In addition, from Eqs. (12) and (A2) we obtain that the upper compensation depth, z_{c1} ,
 252 is the location where the growth limited by nutrients, $\mu_m g(N)$, equals the loss rate,

253 ε , while the lower compensation depth, z_{c2} , represents the depth where the growth
 254 limited by light, $\mu_m f(I)$, equals the loss rate, ε .

255 **3 Results**

256 *3.1 Analytic solutions of three SCM characteristics*

257 By substituting the growth limitation function for light (Eqs. 4 and 5) into Eqs. (14)
 258 or (15), we obtain the expression of parameter z_m , i.e.,

$$259 \quad z_m = \frac{1}{K_d} \ln \left[\left(\frac{\mu_m}{\varepsilon + K_{v2}/\sigma^2} - 1 \right) \frac{I_0}{K_I} \right] \quad (16)$$

260 or

$$261 \quad z_m = \frac{1}{K_d} \ln \left[\left(\frac{\mu_m}{\varepsilon - w/\sigma} - 1 \right) \frac{I_0}{K_I} \right] - \sigma. \quad (17)$$

262 The occurrence for a SCM requires $z_m > 0$. Requiring a positive solution for Eq.
 263 (16), we obtain $\left(\frac{\mu_m}{\varepsilon + K_{v2}/\sigma^2} - 1 \right) \frac{I_0}{K_I} > 1$, i.e., $(\mu_m f(I_0) - \varepsilon)\sigma^2 > K_{v2}$. For any $\sigma > 0$, we
 264 get $\mu_m f(I_0) > \varepsilon$. That is, the necessary condition for the existence of SCM is
 265 $\mu_m f(I_0) > \varepsilon$, which is identical with the result of Fennel and Boss (2003) when
 266 vertical sinking is constant as a function of depth in their model.

267 Subtracting Eqs. (16) and (17), and rearranging, we obtain the expression of
 268 parameter σ :

$$269 \quad \left(\frac{\mu_m}{\mu_m - \varepsilon + \frac{w}{\sigma}} - 1 \right) e^{K_d \sigma} = \frac{\mu_m}{\mu_m - \varepsilon - \frac{K_{v2}}{\sigma^2}} - 1 \quad (18)$$

270 Thus far, we have obtained the theoretical relationships between Gaussian parameter
 271 σ , z_m and environmental parameters (Eqs. 16-18). To derive the relationship between
 272 Gaussian parameter h and environmental parameters, we now return to Eqs. (1) and
 273 (2). In steady state, adding these two equations leads to:

$$274 \quad (1 - \alpha) \varepsilon P + w \frac{dP}{dz} = \frac{d^2}{dz^2} (K_v (P + N)) \quad (19)$$

275 Note that this relationship holds irrespective of the form of growth limiting function.

276 Integrating this equation from the surface to bottom boundary (z_b) and using
 277 boundary conditions (Eq. 6) gives:

$$278 \quad (1-\alpha)\varepsilon\int_0^{z_b} P(z)dz = K_{v2}\left.\frac{dN}{dz}\right|_{z=z_b} \quad (20)$$

279 When the recycling processes do not immediately convert dead phytoplankton back
 280 into dissolved nutrients below the surface mixed layer, i.e., $\alpha \neq 1$ (For $\alpha = 1$, the
 281 detailed derivation for the intensity of SCML is presented at Appendix B), one gets
 282 the total Chl a in the water column:

$$283 \quad h = \frac{K_{v2}\left.\frac{dN}{dz}\right|_{z=z_b}}{(1-\alpha)\varepsilon} \quad (21)$$

284 The intensity of SCML is

$$285 \quad P_{\max} = \frac{K_{v2}\left.\frac{dN}{dz}\right|_{z=z_b}}{\sqrt{2\pi}\sigma(1-\alpha)\varepsilon} \quad (22)$$

286 Obviously, both the total Chl a in the water column and the intensity of SCML are
 287 proportional to the flux of nutrients from below ($K_{v2}\left.\frac{dN}{dz}\right|_{z=z_b}$), which is determined
 288 by the diffusivity below the surface mixed layer and the nutrients gradient at the
 289 bottom of water column. Varela et al. (1994) also found a similar result by
 290 simulations.

291 *3.2 Influences of environmental parameters on SCM characteristics*

292 We now investigate how the steady-state thickness, depth, and intensity of SCML
 293 depend on environmental parameters. Because the analytic solutions for SCML depth
 294 and intensity depend on Gaussian parameter σ and environmental parameters, we first
 295 examine the influence of environmental parameters on parameter σ .

296 Equation (18) shows that the thickness of SCML is independent of sea surface light
 297 intensity (I_0). This is consistent with numerical simulations (Beckmann and Hense,
 298 2007). This result also suggests that seasonal variation of SCML thickness has no
 299 relation with light intensity. Thus, it is not surprising that the empirical model poorly
 300 predicted parameter σ by using season as an important factor (Richardson et al.,
 301 2003).

302 To illustrate the effects of other model parameters (K_d , K_{v2} , μ_m , ε , w) on the parameter
 303 σ , we need to obtain informative algebraic expression of σ . To simplify, by Taylor
 304 expanding $e^{K_d\sigma}$ at $\sigma=0$ and truncating the Taylor series after the linear term, i.e.,
 305 $e^{K_d\sigma} = 1 + K_d\sigma + o(\sigma^2)$, Eq. (18) can thereby be rewritten as:

$$306 \quad \sigma^3 - \frac{w}{\varepsilon}\sigma^2 - \frac{\varepsilon K_d K_{v2} + \mu_m w}{\varepsilon K_d (\mu_m - \varepsilon)}\sigma = \frac{K_{v2}(\mu_m/K_d - w)}{\varepsilon(\mu_m - \varepsilon)}. \quad (23)$$

307 According to the properties of a cubic function, we know that Eq. (23) has one and
 308 only one positive real root σ , when $\frac{K_{v2}(\mu_m/K_d - w)}{\varepsilon(\mu_m - \varepsilon)} \geq 0$. Because $\mu_m f(I_0) > \varepsilon$ and
 309 $0 < f(I_0) < 1$, so $\mu_m > \varepsilon$. Thus, when the maximum phytoplankton growth rate (μ_m)
 310 within one penetration depth ($1/K_d$) is larger than sinking velocity of phytoplankton,
 311 i.e., $\mu_m/K_d - w \geq 0$, there exists a non-negative value of parameter σ , which
 312 increases with increasing $\frac{K_{v2}(\mu_m/K_d - w)}{\varepsilon(\mu_m - \varepsilon)}$.

313 Using dimensional analysis, Klausmeier and Litchman (2001) found that the degree
 314 of turbulence determines the thickness of SCML. Our analytical result shows that the
 315 thickness of SCML increases with increasing vertical diffusivity below the surface
 316 mixed layer (K_{v2}). In addition, the SCML thickness decreases with increasing sinking
 317 velocity of phytoplankton (w) and light attenuation coefficient (K_d).

318 The right hand term in Eq. (23), $\frac{K_{v2}(\mu_m/K_d - w)}{\varepsilon(\mu_m - \varepsilon)}$, can be rearranged as

$$319 \quad \frac{K_{v2}(\mu_m/K_d - w)}{-(\varepsilon - \mu_m/2)^2 + \mu_m^2/4}. \text{ Thus, the effect of loss rate } (\varepsilon) \text{ on parameter } \sigma \text{ depends on } \mu_m/2.$$

320 Note that $\mu_m f(I_0) > \varepsilon$ once the SCM occurs. When the surface light intensity I_0 is
 321 smaller than or equals to the half-saturation constant for light K_I , i.e., $f(I_0) \leq 0.5$,
 322 then $0 < \varepsilon < \mu_m f(I_0) \leq \mu_m/2$, thus, σ decreases with increasing ε . Conversely, when
 323 $f(I_0) > 0.5$, for $\varepsilon \geq \mu_m/2$, σ increases with increasing ε ; for $\varepsilon < \mu_m/2$, σ decreases
 324 with increasing ε . In summary, for smaller loss rates ($\varepsilon < \mu_m/2$), decreased ε leads to
 325 a thicker SCML, while for larger loss rates ($\varepsilon \geq \mu_m/2$), decreased ε leads to a thinner
 326 SCML.

327 Equation (16) can be rewritten as:

328

$$z_m = \frac{1}{K_d} \ln(AI_0), \quad (24)$$

329 where $A = \frac{1}{K_I} \left(\frac{\mu_m}{\varepsilon + K_{v2}/\sigma^2} - 1 \right)$. Clearly, from Eq. (18) we know A does not depend on

330 surface light intensity (I_0), thus we infer that the depth of SCML increases
 331 logarithmically with increasing I_0 . In other words, the SCML gets deeper due to the
 332 seasonal increase of I_0 , and remains almost unchanged when the surface light
 333 intensity increases to a certain degree. Observations at the HOT (Hawaii Ocean
 334 Time-series) site in the eastern Pacific and the SEATS (South East Asia Time-series
 335 Station) station in the South China Sea showed a significant seasonal variation of
 336 SCML depth (Chen et al., 2006; Hense and Beckmann, 2008). Hense and Beckmann
 337 (2008) explained the deepening of SCML depth in spring at HOT site by the seasonal
 338 increase of the light intensity. Modeling sensitivity analyses also showed that an
 339 increase in the surface light intensity yields a deeper SCML (Jamart et al., 1979;
 340 Varela et al., 1994; Beckmann and Hense, 2007).

341 Determining the effect of vertical diffusivity below the surface mixed layer (K_{v2}) on
 342 the steady-state SCML intensity is more difficult. Increased K_{v2} increases parameter
 343 σ (Eq. 23) and the diffusive flux of nutrients from below (Eq. 22), however, this
 344 parameter has opposite effects on P_{\max} (Eq. 22). Rearranged Eq. (23) we obtain

$$345 \quad \frac{K_{v2}}{\sigma} = \frac{(\mu_m - \varepsilon)\varepsilon}{(\mu_m/K_d - w)/\sigma^2 + \varepsilon/\sigma} + \frac{(\mu_m - \varepsilon)w}{(\mu_m/K_d - w)/\sigma + \varepsilon} - \frac{\mu_m w/K_d}{\mu_m/K_d - w + \varepsilon\sigma}. \quad (25)$$

346 Clearly, all the three terms in the right hand of this equality increase due to the
 347 increasing σ by a higher K_{v2} . Therefore, it can be inferred that increased vertical
 348 diffusivity below the surface mixed layer (K_{v2}) leads to a stronger SCML intensity
 349 (P_{\max}).

350 The influences of various parameters on SCM characteristics determined by Eqs.
 351 (16)-(18), (21) and (22) are summarized in Table 1. For example, increased light
 352 levels (increasing surface light intensity I_0 , decreasing attenuation coefficient K_d) or
 353 increased light competitive ability (decreasing half-saturation constant for light K_I)
 354 moves the SCML deeper; increased nutrients supply (increasing vertical diffusivity
 355 below the surface mixed layer K_{v2} and loss rate of phytoplankton ε) moves the layer
 356 toward the surface. The shape of SCML (thickness and intensity) is mainly

357 influenced by nutrients supply (K_{v2} and ε). The intensity of SCML becomes weaker
358 as a result of expanding the SCML by a lower sinking velocity of phytoplankton (w)
359 and a smaller light attenuation coefficient (K_d).

360 **4 Discussion**

361 Considering the two compartment system (nutrients and Chl a) in steady state and a
362 general Gaussian function for vertical Chl a concentration, we derived the analytical
363 solution for the fundamental relationships between SCM characteristics and various
364 parameters. Three special sceneries, limitation and implications of this study were
365 discussed below.

366 *4.1 Three special sceneries*

367 Equation (18) indicates that the parameter σ is affected by changes in the vertical
368 diffusivity below the surface mixed layer (K_{v2}), the sinking velocity of phytoplankton
369 (w) and the light attenuation coefficient (K_d), which inversely affects depth and
370 intensity of SCML (Eqs. 16, 17, and 22). Thus, three special situations of the
371 theoretical solutions for SCM characteristics are discussed below.

372 Firstly, the term K_{v2}/σ^2 in the right hand of Eq. (18) is neglected. This special
373 situation occurs either when the vertical diffusivity below the surface mixed layer is
374 too small to be considered ($K_{v2} \rightarrow 0$), or when K_{v2}/σ^2 is much smaller than $\mu_m - \varepsilon$,
375 i.e., the mixing time scale ($T = \sigma^2/K_{v2}$) below the surface mixed layer is much longer
376 than the time taken by net growth of phytoplankton, $(\mu_m - \varepsilon)^{-1}$. Indeed, in the
377 seasonal thermocline, vertical turbulent diffusive time scales can vary from weeks to
378 months for phytoplankton displacements as small as several meters (Denman and
379 Gargett, 1983). The value of $(\mu_m - \varepsilon)^{-1}$ used in many studies is usually from 0.1 to 5
380 days (Gabric and Parslow, 1989; Klausmeier and Litchman, 2001; Huisman et al.,
381 2006).

382 In this situation, from Eq. (14), the growth rate at SCML depth can be expressed as:

$$383 \quad \mu_m f(I)|_{z=z_m} = \varepsilon. \quad (26)$$

384 In regions with a low vertical diffusivity, Fennel and Boss (2003) derived that, at the
385 SCML depth, the growth rate of phytoplankton is equal to the loss rate and the
386 divergence of phytoplankton due to changes in the sinking velocity. Clearly, Eq. (26)

387 is identical to that of Fennel and Boss (2003) for constant sinking velocity of
388 phytoplankton.

389 In this situation, the depth of SCML can be derived from Eq. (16), i.e.,

$$390 \quad z_m = \frac{1}{K_d} \ln \frac{(\mu_m - \varepsilon) I_0}{\varepsilon K_I}. \quad (27)$$

391 It indicates the SCML depth is directly proportional to the light penetration depth
392 ($1/K_d$). Beckmann and Hense (2007) have found a similar result by statistical analysis
393 of numerical modeling.

394 The right hand term of Eq. (27) can be rewritten as $\frac{1}{K_d} \ln \frac{I_0}{I^*}$ by letting $I^* = \frac{\varepsilon K_I}{\mu_m - \varepsilon}$,
395 where $\mu_m f(I^*) = \varepsilon$. Under the assumption of infinitely thin SCML ($\sigma \rightarrow 0$),
396 Klausmeier and Litchman (2001) also have derived Eq. (27) by setting the vertical
397 diffusivity for phytoplankton as zero, i.e., $K_v = 0$, in poorly mixed waters. Here, we
398 go further to obtain the approximate expression of the thickness of SCML from Eq.
399 (23), that is,

$$400 \quad 2\sigma = \frac{w}{\varepsilon} + \sqrt{\left(\frac{w}{\varepsilon}\right)^2 + \frac{w}{K_d(\varepsilon - \varepsilon^2/\mu_m)}}. \quad (28)$$

401 Obviously, the thickness of SCML increases with an increase in the sinking velocity
402 of phytoplankton (w), and with a decrease in the maximal growth rate (μ_m) and the
403 light attenuation coefficient (K_d).

404 The second special situation occurs when the term w/σ in the left hand of Eq. (18) is
405 neglected. This special case occurs in regions where phytoplankton sinking velocity
406 is very low ($w \rightarrow 0$), or when w/σ is much smaller than $\mu_m - \varepsilon$, i.e., the time taken by
407 phytoplankton sinking through half-length of SCML, $(w/\sigma)^{-1}$, is much longer than the
408 time taken by net growth of phytoplankton, $(\mu_m - \varepsilon)^{-1}$. Phytoplankton sinking
409 velocities exhibit a range of values depending on physical and physiological
410 phenomena (e.g., size and shape of the cell). In the environment, estimates of sinking
411 velocity vary from 0 to 9 m per day (Gabric and Parslow, 1989; Huisman and
412 Sommeijer, 2002). Thus, the latter special scenarios (i.e., $w/\sigma \ll \mu_m - \varepsilon$) can indeed
413 occur.

414 In this situation, according to Eq. (15), the net growth rate at the lower boundary of
 415 SCML can be expressed as

$$416 \quad \mu_m f(I)|_{z=z_m+\sigma} - \varepsilon = 0. \quad (29)$$

417 That is, the lower boundary of SCML, $z_m+\sigma$, is located at the compensation depth.

418 In this situation, the depth of SCML can be derived from Eq. (17), i.e.,

$$419 \quad z_m = \frac{1}{K_d} \ln \frac{(\mu_m - \varepsilon) I_0}{\varepsilon K_l} - \sigma. \quad (30)$$

420 Compared with Eq. (27), we know that the depth of SCML is shallower in this special
 421 case than that in the case of neglecting the influence of vertical diffusivity below the
 422 surface mixed layer on SCM. This result implies that the displacement (σ) of SCML
 423 depth is the result of combined influences of vertical diffusivity and sinking velocity
 424 of phytoplankton.

425 In this situation, from Eq. (23), we have

$$426 \quad \sigma \left(\sigma + \sqrt{\frac{K_{v2}}{\mu_m - \varepsilon}} \right) \left(\sigma - \sqrt{\frac{K_{v2}}{\mu_m - \varepsilon}} \right) = \frac{\mu_m K_{v2}}{(\mu_m - \varepsilon) \varepsilon K_d}. \quad (31)$$

427 The SCML thickens with a larger vertical diffusivity below the surface mixed layer
 428 (K_{v2}), a smaller growth rate (μ_m) or a lower light attenuation coefficient (K_d).
 429 Especially, when $K_{v2} = 0$, we have $\sigma = 0$. In other words, for non-sinking
 430 phytoplankton ($w \rightarrow 0$), when the vertical diffusivity below the surface mixed layer is
 431 very small ($K_{v2} \rightarrow 0$), the SCML disappears. This indicates that there must be a
 432 vertical diffusion window sustaining non-sinking phytoplankton species in deep
 433 waters.


434 The third special situation occurs when $K_d \sigma$ (i.e., $\sigma / (K_d)^{-1}$) is too small to be
 435 considered in Eq. (18). This may occur in clear waters where the light attenuation
 436 coefficient is very small ($K_d \rightarrow 0$), or in regions where the light penetration depth
 437 ($1/K_d$) is much larger than a half-width of SCML (σ). Very narrow (from several to
 438 tens of centimeters) SCML has been observed in clear, stratified lakes where the light
 439 penetration depths were from several to tens of meters (Fee, 1976; Camacho, 2006).

440 In this situation, Eq. (18) can be modified to

441 $w\sigma + K_{v2} = 0.$ (32)

442 Clearly, when $K_{v2} = 0$, $w=0$, this equation has infinitely many solutions. This means
443 in stable, clear waters with a predominance of small cells, the deep SCML can occur
444 with different thicknesses. For example, in the basin of South China Sea, $<3 \mu\text{m}$
445 phytoplankton (such as *Prochlorococcus*, *Synechococcus*, picoeukaryotes, etc.) are
446 the dominant species in SCMLs (Takahashi and Hori, 1984; Liu et al., 2007) with
447 variable thicknesses (Lee Chen, 2005; Chen et al., 2006).

448 *4.2 Limitation and potential application*

449 To make the complex problem (SCM phenomenon) tractable, the ecosystem
450 dynamical equations adopted in this study are judiciously simplified. For example, a
451 constant eddy diffusivity is assumed in the surface mixed layer and below this layer,
452 respectively. Many processes (turbulence, internal waves, storms, slant-wise and
453 vertical convection) in upper ocean dynamics are not captured in the model system.
454 The assumption of steady state will be broken during episodic events of strong
455 physical forcing, nutrient injection, or blooms (Fennel and Boss, 2003). Similarly the
456 biological representation is also extremely limited. We neglect food-web and
457 microbial loop dynamics (detritus, dissolved organic matter, and zooplankton are not
458 included explicitly), and assume all loss processes, except sinking, to be linearly
459 proportional to phytoplankton. The sinking velocity of phytoplankton is assumed to
460 be constant with depths, excluding the effects of temperature and density gradients.
461 Our model also neglects some feedback mechanisms, like the effect of phytoplankton
462 on light attenuation. Although these are important aspects that could be included,
463 their addition is unlikely to change our conclusions qualitatively (Fennel and Boss,
464 2003). 

465 In a stratified water column with a well-mixed surface layer on top of a poorly mixed
466 subsurface layer, a general Gaussian function of vertical Chl a profile represents the
467 distribution of which the surface Chl a concentration is nearly zero, the maximum of
468 Chl a is significantly deeper than the base of surface mixed layer, and the vertical
469 gradient of Chl a is identically zero at the transition between the two layers. The
470 assumption of a general Gaussian profile can be broken in several ways. If nutrient
471 input to the mixed layer due to riverine inputs, surface runoff, or atmospheric
472 deposition, was considered in the ecosystem, then the surface concentration of Chl a

473 should be positive (Mellard et al. 2011). If the depth of surface mixed layer z_s is large,
474 this allows another way for the surface Chl a concentration being positive by
475 extracting some of the Chl a from the SCML (Beckman and Hense, 2007), then the
476 vertical gradient of Chl a may not be identically zero at the transition between the
477 two layers.

478 Under the assumption of a constant loss rate, the lower compensation depth we got
479 from Eq. (11), the location where the growth rate of phytoplankton limited by light
480 equals the loss rate, is similar to the popular definition of compensation depth given
481 by Sverdrup (1953), below which no net growth occurs. This assumption is in the
482 heart of the Sverdrup's critical depth model and we now understand that it has
483 significant limitations (Behrenfeld and Boss, 2014). Particularly, the treatment of
484 grazing loss, is, in the least, an oversimplification, though many numerical models
485 used a similar one (e.g., Klausmeier and Litchman, 2001; Fennel and Boss, 2003;
486 Huisman et al., 2006). Grazing loss depends strongly on C_a concentration (it is an
487 encounter based process) and, given that zooplankton can move, or, in the least, grow
488 faster where more food is available, is unlikely to have a constant concentration
489 distribution (Behrenfeld and Boss, 2014).

490 Our model suggests that the condition for the existence of a SCM is the growth rate
491 under the limitation of light intensity, $\mu_m f(I_0)$, is larger than the loss rate, ε , in
492 stratified water columns. Fennel and Boss (2003) found a similar result and pointed
493 out that this condition for a SCM is general. Many numerical studies have reproduced
494 the SCM phenomenon, of which the condition of SCM occurrence met with variable
495 values of the sinking velocity of phytoplankton and the mixing diffusivity
496 (Klausmeier and Litchman, 2001; Huisman et al., 2006; Mellard et al., 2011).

497 Our two compartment system model reproduces some of the results of the more
498 complex model with three compartments (phytoplankton, nutrients, and detritus,
499 Beckmann and Hense, 2007). For example, our model predicts that with fully
500 recycling of the dead phytoplankton, the total Chl a concentration in water columns
501 depends on the sinking velocity of phytoplankton and the vertical diffusivity, but
502 independent on the growth rate and the loss rate of phytoplankton. Beckmann and
503 Hense (2007) found similar results. Here, we go further to point out an interesting
504 finding that the derivations of the total Chl a are irrespective of the form of the

505 growth limiting function. Since growth functional forms in phytoplankton models are
506 still debated in the literature (Haney, 1996; Ayata et al., 2013), this will be most
507 helpful to estimate the vertical integrated Chl a and primary production.

508 The relationships (in previous sections and in Appendices A and B) we derived can
509 be used to compute missing model parameters (such as maximum growth rate μ_m ,
510 loss rate ε , recycling rate α) which are difficult to obtain by on-site observation, if
511 estimates of others are available. For example, Eq. (B4) allows us to obtain an
512 estimate of the sinking velocity of phytoplankton from the measurement of SCM
513 thickness and intensity, the nutrient concentration at water column depth, and the
514 vertical diffusivity below the surface mixed layer.

515 Our analytic solutions can in principle be tested through a comparison with
516 observations: for example, the shape of profiles (the SCML thickness, depth, and
517 intensity), expressed by the characteristic relationships (Eqs. 16-18, 22 and B4), the
518 vertical integral of total subsurface Chl a concentration (Eqs. 21 and B3), the
519 consistency of independent field estimates for sinking velocity, vertical diffusivity,
520 recycling rate and loss rate (Eqs. 21-22 and B3-B4).

521 We retrieve the three SCM characteristics from Eqs. (16-18, and 22) by combining
522 remote sensing data (annual averaged values of surface light intensity I_0 and light
523 attenuation coefficient K_d) and some parameters from published field and numerical
524 studies (e.g., sinking velocity of phytoplankton w , vertical diffusivity below the
525 surface mixed layer K_{v2} , loss rate ε , maximum growth rate μ_m). Table 2 lists the
526 values of model parameters at three time-series stations in different ocean regions, i.e.,
527 the SEATS station, the HOT station, and the Bermuda Atlantic Time-Series Study
528 (BATS) site in the Sargasso Sea, and the corresponding references. The estimated
529 results and the observed values of the SCML thickness, depth and intensity at the
530 three stations are shown in Fig. 2.

531 The estimated depths and thicknesses of the SCML agree reasonably well with the
532 observations at all three stations. However, the intensities of the SCML are poorly
533 estimated, implying that other mechanisms supplying nutrients for the SCML, except
534 upward diffusivity, for phytoplankton growth (Williams et al., 2013). This is the first
535 try to estimate the depth, thickness and intensity of the SCML using parameters from
536 satellite data and field studies. We note that the kinematic solution assumed (Eq. 7) is,

537 at best, an approximate solution of the dynamical Eqs. (1-2). Even though
538 disagreements could be associated with uncertainties from several sources, this type
539 of try would give some idea of how real-world data could be incorporated into the
540 model and thus be applied to the field (Pitarch et al. 2014).

541 **5 Summary**

542 A general Gaussian function is assumed to represent a bell-shape vertical distribution
543 of Chl a in stratified water columns. The function is incorporated into the ecosystem
544 dynamical equations to determine three steady-state SCM characteristics and examine
545 their dependence on environmental parameters such as vertical diffusivity, sinking
546 velocity of phytoplankton, light attenuation coefficient.

547 The maximum Chl a concentration occurs at or below the location of the maximum
548 growth rates of phytoplankton determined by the vertical mixing time scale and the
549 time taken by a phytoplankton sinking through the length scale.

550 The depth of the SCML in steady state deepens logarithmically with an increase in
551 surface light intensity, but shoals with increasing light attenuation coefficient,
552 increasing vertical diffusivity below the surface mixed layer, increasing loss rate of
553 phytoplankton, and with decreasing sinking velocity of phytoplankton.

554 The shape of the SCML (thickness and intensity) is mainly influenced by nutrients
555 supply, but independent of sea surface light intensity. The SCML gets thicker and
556 stronger with a higher vertical diffusivity below the surface mixed layer. The
557 intensity of SCML in steady state weakens as a result of expanding the SCML by a
558 smaller sinking velocity of phytoplankton and a lower light attenuation coefficient.

559 In regions with a low vertical diffusivity, the SCML depth is inversely proportional to
560 light attenuation coefficient, and is deeper than that in regions dominated by
561 non-sinking phytoplankton. In clear and stable waters with a predominance of small
562 cells, deeper SCMLs can occur with different thicknesses.

563 Upon potential risk of climate change, it is critical to accurately estimate the global
564 and regional SCML-related primary production. However, the SCM characteristics
565 cannot be detected by remote sensing satellites, which will restrict the application of
566 satellite data in estimating primary production in a large temporal and spatial scale.
567 The relationships we derived might help to estimate depth-integrated primary
568 production using available data from satellite observations (incident light and light

569 attenuation coefficient) when appropriate vertical estimates of growth rate and loss
570 rate of phytoplankton, sinking velocity of phytoplankton and vertical diffusivity were
571 adopted based on observations or model results. Again, the solutions could also help
572 to compute environmental parameters that are difficult to obtain from on-site
573 observation.

574

575 **Appendix A**

576 In steady state, the net nutrient flux at any given depth (z) is equals to the net
 577 nutrients consumption by phytoplankton, then from steady-state of Eq. (2) we obtain
 578 Eq. (A1) below the surface mixed layer:

$$579 \quad \int (\mu_m \min(f(I), g(N)) - \alpha \varepsilon) P(z) dz \approx K_{v2} \frac{dN(z)}{dz} \Big|_z \quad (\text{A1})$$

580 If $\mu_m \min(f(I), g(N)) - \varepsilon > 0$, then $\mu_m \min(f(I), g(N)) - \alpha \varepsilon > 0$ for $0 < \alpha \leq 1$, we will
 581 have $\frac{dN}{dz} > 0$. That is, $N(z)$ will increase with depth below the surface mixed layer.

582 From the properties of the quadratic function in the right hand of Eq. (10), we have
 583 $\mu_m \min(f(I), g(N)) - \varepsilon > 0$ on the interval (z_{c1}, z_{c2}) . Hence, we have
 584 $\mu_m \min(f(I), g(N)) - \alpha \varepsilon > 0$ for $0 < \alpha \leq 1$, then $dN/dz > 0$. In other words, $N(z)$
 585 increases with depth on the interval (z_{c1}, z_{c2}) .

586 According to Eq. (4), we know that $g(N)$ is a monotonic increasing function on
 587 interval (z_{c1}, z_{c2}) , and $f(I)$ is a monotonic decreasing function on interval (z_{c1}, z_{c2}) .
 588 Note that we have known that the stable SCML occurs in stratified water column only
 589 when the growth of phytoplankton in the surface mixed layer is nutrient-limited
 590 (Mellard et al., 2011; Ryabov et al., 2010). In other words, the limitation by nutrients
 591 $g(N)$ is less than the limitation by light $f(I)$ within the surface mixed layer, i.e., $g(N) <$
 592 $f(I)$ for $0 \leq z \leq z_s$.

593 Because there is only one maximum in the growth rates of phytoplankton which
 594 occurs at the depth $z_0 = z_m - \frac{w\sigma^2}{2K_{v2}}$, and $z_{c1} < z_0 < z_{c2}$ (Eq. 11), we arrive at

$$595 \quad \min(f(I), g(N)) = \begin{cases} g(N) & z_{c1} \leq z \leq z_0 \\ f(I) & z_0 \leq z \leq z_{c2} \end{cases} \quad (\text{A2})$$

596 and

$$597 \quad \max(\mu_m \min(f(I), g(N))) = \mu_m f(I) \Big|_{z=z_0} \quad (\text{A3})$$

598 That is, the maximum growth rate occurs at the depth z_0 where is the transition

599 from nutrients limitation to light limitation, and the growth of phytoplankton is
600 light-limited below the depth z_0 .

601 **Appendix B**

602 The dead phytoplankton is entirely recycled ($\alpha = 1$), and thus the system is closed. In
603 this case, at steady state Eq. (19) reduces to

604
$$w \frac{dP}{dz} = \frac{d^2}{dz^2} (K_v (P + N)) \quad (\text{B1})$$

605 Integrating this equation twice from the surface to bottom boundary (z_b) and using
606 boundary conditions (Eq. 6) gives

607
$$w \int_0^{z_b} P(z) dz = K_{v1} (P + N) \Big|_0^{z_s} + K_{v2} (P + N) \Big|_{z_s+0}^{z_b} \quad (\text{B2})$$

608 Note that we have known that the SCML occurs only when the growth of
609 phytoplankton within the surface mixed layer is nutrient-limited, then we further
610 assume the surface nutrients value is negligible. Using the assumption of small Chl a
611 at the top and the bottom boundaries of the model domain, we obtain

612
$$h = \frac{K_{v2}}{w} N(z_b) \quad (\text{B3})$$

613 and the intensity of SCML is

614
$$P_{\max} = \frac{K_{v2}}{\sqrt{2\pi\sigma w}} N(z_b) \quad (\text{B4})$$

615 where $N(z_b)$ is the nutrients concentration at depth z_b . Therefore, with $\alpha = 1$, the
616 intensity of SCML is affected by the ambient nutrients concentration below the
617 surface mixed layer. The total Chl a in the water column depends on the sinking
618 velocity of phytoplankton and the diffusivity, but it is independent on the growth rate
619 and loss rate of phytoplankton. Analogous results have been obtained by Liccardo et
620 al. (2013). Beckmann and Hense (2007) also found similar result by introducing an
621 explicit compartment for the detritus in their models.

622 **Acknowledgements.** We gratefully acknowledge E. Boss, J. Pitarch, and two
623 anonymous reviewers for constructive and insightful reviews. We also thank
624 particularly X. H. Liu and Z. Y. Cai for programming assistance and precious advice.
625 This work is funded in part by the National Key Basic Research Program of China
626 under the contract 2014CB953700, the National Nature Science Foundation of China
627 under the contract (41406010, 41210008, 41106007), and the China Postdoctoral
628 Science Foundation under the contract 2013M541958.

References:

- 630 Anderson, G. C.: Subsurface chlorophyll maximum in the northeast Pacific Ocean, *Limnol. Oceanogr.*,
631 14, 386-391, 1969.
- 632 Ardyna, M., Babin, M., Gosselin, M., Devred, E., Bélanger, S., Matsuoka, A., Tremblay, J. E.:
633 Parameterization of vertical chlorophyll a in the Arctic Ocean: impact of the subsurface chlorophyll
634 maximum on regional, seasonal and annual primary production estimates, *Biogeosciences*, 10,
635 4383-4404, doi: 10.5194/bg-10-4383-2013, 2013.
- 636 Ayata, S., Lévy, M., Aumont, O., Sciandra, A., Sainte-Marie, J., Tagliabue, A., Bernard, O.:
637 Phytoplankton growth formulation in marine ecosystem models: should we take into account
638 photo-acclimation and variable stoichiometry in oligotrophic areas? *J. Marine Syst.*, 125, 29-40, 2013.
- 639 Beckmann, A., Hense, I.: Beneath the surface: Characteristics of oceanic ecosystems under weak
640 mixing conditions-A theoretical investigation, *Prog. Oceanogr.*, 75, 771-796, 2007.
- 641 Behrenfeld, M. J., Boss, E. S.: Resurrecting the ecological underpinnings of ocean plankton blooms,
642 *Annu. Rev. Mar. Sci.*, 6, 167-194, 2014.
- 643 Bienfang, P. K., Harrison, P. J.: Sinking-rate response of natural assemblages of temperate and
644 subtropical phytoplankton to nutrient depletion, *Mar. Biol.*, 83, 293-300, 1984.
- 645 Bowdon, K. F.: Physical oceanography of coastal waters. *Limnol. Oceanogr.*, 30, 449-450, 1985.
- 646 Cai Y. M., Ning X. R., Liu C. G.: *Synechococcus* and *Prochlorococcus* growth and mortality rates in
647 the northern China Sea: range of variations and correlation with environmental factors. *Acta Ecol. Sin.*
648 7, 2237-2246, 2006.
- 649 Camacho, A.: On the occurrence and ecological features of deep chlorophyll maxima (DCM) in
650 Spanish stratified lakes, *Limnetica*, 25, 453-478, 2006.
- 651 Chen, C. C., Shiah, F. K., Chung, S. W., Liu, K. K.: Winter phytoplankton blooms in the shallow
652 mixed layer of the South China Sea enhanced by upwelling, *J. Marine Syst.*, 59, 97-110, 2006.
- 653 Cianca, A., Godoy, J. M., Martin, J. M., Perez Marrero, J., Rueda, M. J., Llinás, O., Neuer, S.:
654 Interannual variability of chlorophyll and the influence of low - frequency climate models in the North
655 Atlantic subtropical gyre, *Global Biogeochem. Cy.*, 26, 2012.
- 656 Cianca, A., Helmke, P., Mouriño, B., Rueda, M. J., Llinás, O., Neuer, S.: Decadal analysis of
657 hydrography and in situ nutrient budgets in the western and eastern North Atlantic subtropical gyre, *J.*
658 *Geophys. Res.*, 112, C07025, 1-18, 2007.
- 659 Cloern, J. E., Grenz, C., Videgar-Lucas, L.: An empirical model of the phytoplankton chlorophyll:
660 carbon ratio-the conservation factor between productivity and growth rate, *Limnol. Oceanogr.*, 40,
661 1313-1321, 1995.
- 662 Cullen, J. J., Eppley, R. W.: Chlorophyll maximum layers of the Southern California Bight and
663 possible mechanisms of their formation and maintenance, *Oceanol. Acta*, 1, 23-32, 1981.
- 664 Cullen, J. J.: The deep chlorophyll maximum: comparing vertical profiles of chlorophyll a, *Can. J. Fish.*
665 *Aquat. Sci.*, 39, 791-803, 1982.
- 666 Dekshenicks, M. M., Donaghay, P. L., Sullivan, J. M., Rines, J. E., Osborn, T. R., Twardowski, M. S.:
667 Temporal and spatial occurrence of thin phytoplankton layers in relation to physical processes, *Mar.*
668 *Ecol-Prog. Ser.*, 223, 61-71, 2001.
- 669 Denman, K. L., Gargett, A. E.: Time and space scales of vertical mixing and advection of
670 phytoplankton in the upper ocean, *Limnol. Oceanogr.*, 28, 801-815, 1983.
- 671 Fee, E. J.: The vertical and seasonal distribution of chlorophyll in lakes of the Experimental Lakes Area,
672 northwestern Ontario: Implications for primary production estimates. *Limnol. Oceanogr.*, 26, 767-783,
673 1976.
- 674 Fennel, K., Boss, E.: Subsurface maxima of phytoplankton and chlorophyll: Steady-state solutions
675 from a simple model, *Limnol. Oceanogr.*, 48, 1521-1534, 2003.

676 Gabric, A. J., Parslow, J.: Effect of physical factors on the vertical distribution of phytoplankton in
677 eutrophic coastal waters, *Aust. J. Mar. Fishwater Res.*, 40, 559-569, 1989.

678 Ghosal, S., Mandre, S.: A simple model illustrating the role of turbulence on phytoplankton blooms, *J.*
679 *Math. Biol.*, 46, 333-346, 2003.

680 Haney, J. D.: Modeling phytoplankton growth rates, *J. Plankton Res.*, 18, 63-85, 1996.

681 Hanson, C. E., Pesant, S., Waite, A. M., Pattiaratchi, C. B.: Assessing the magnitude and significance
682 of deep chlorophyll maxima of the coastal eastern Indian Ocean, *Deep-Sea Res. Pt. II*, 54, 884-901,
683 2007.

684 Hense, I., Beckmann, A.: Revisiting subsurface chlorophyll and phytoplankton distributions, *Deep-Sea*
685 *Res. Pt. I*, 55, 1193-1199, 2008.

686 Hodges, B. A., Rudnick, D. L.: Simple models of steady deep maxima in chlorophyll and biomass,
687 *Deep-Sea Res. Pt. I*, 51, 999-1015, 2004.

688 Hood, R. R., Bates, N. R., Capone, D. G., Olson, D. B.: Modeling the effect of nitrogen fixation on
689 carbon and nitrogen fluxes at BATS, *Deep-Sea Res. Pt. II*, 48, 1609-1648, 2001.

690 Huisman, J., Sommeijer, B.: Maximal sustainable sinking velocity of phytoplankton, *Mar. Ecol.-Prog.*
691 *Ser.*, 244, 39-48, 2002.

692 Huisman, J., Thi, N., Karl, D. M., Sommeijer, B.: Reduced mixing generates oscillations and chaos in
693 the oceanic deep chlorophyll maximum, *Nature*, 439, 322-325, 2006.

694 Jamart, B. M., Winter, D. F., Banse, K.: Sensitivity analysis of a mathematical model of phytoplankton
695 growth and nutrient distribution in the Pacific Ocean off the northwestern US coast, *J. Plankton Res.*, 1,
696 267-290, 1979.

697 Klausmeier, C. A., Litchman, E.: Algal games: The vertical distribution of phytoplankton in poorly
698 mixed water columns, *Limnol. Oceanogr.*, 8, 1998-2007, 2001.

699 Lee Chen, Y.: Spatial and seasonal variations of nitrate-based new production and primary production
700 in the South China Sea, *Deep-Sea Res. Pt. I*, 52, 319-340, 2005.

701 Lewis, M. R., Cullen, J. J., Platt, T.: Phytoplankton and thermal structure in the upper ocean:
702 consequences of nonuniformity in chlorophyll profile, *J. Geophys. Res.*, 88, 2565-2570, 1983.

703 Lewis, M. R., Harrison, W. G., Oakey, N. S., Hebert, D., Platt, T.: Vertical nitrate fluxes in the
704 oligotrophic ocean, *Science*, 234, 870-873, 1986.

705 Liccardo, A., Fierro, A., Iudicone, D., Bouruet-Aubertot, P., Dubroca, L.: Response of the Deep
706 Chlorophyll Maximum to fluctuations in vertical mixing intensity, *Prog. Oceanogr.*, 2013, 33-46, 2013.

707 Liu, H., Chang, J., Tseng, C. M., Wen, L. S., Liu, K. K.: Seasonal variability of picoplankton in the
708 Northern South China Sea at the SEATS station, *Deep-Sea Res. Pt. II*, 54, 1602-1616, 2007.

709 Lu, Z., Gan, J., Dai, M., Cheung, A.: The influence of coastal upwelling and a river plume on the
710 subsurface chlorophyll maximum over the shelf of the northeastern South China Sea, *J. Marine Syst.*,
711 82, 35-46, 2010.

712 Mara On, E., Holligan, P. M.: Photosynthetic parameters of phytoplankton from 50° N to 50° S in the
713 Atlantic Ocean, *Mar. Ecol.-Prog. Ser.*, 176, 191-203, 1999.

714 Mellard, J. P., Yoshiyama, K., Litchman, E., Klausmeier, C. A.: The vertical distribution of
715 phytoplankton in stratified water columns, *J. Theor. Biol.*, 269, 16-30, 2011.

716 Morel, A.: Optical modeling of the upper ocean in relation to its biogenous matter content (case I
717 waters), *J. Geophys. Res.*, 93, 749-768, 1988.

718 Ono, S., Ennyu, A., Najjar, R. G., Bates, N. R.: Shallow remineralization in the Sargasso Sea estimated
719 from seasonal variations in oxygen, dissolved inorganic carbon and nitrate, *Deep-Sea Res. Pt. II*, 48,
720 1567-1582, 2001.

721 Oschlies, A.: Model-derived estimates of new production: New results point towards lower values,
722 *Deep-Sea Res. Pt. II*, 48, 2173-2197, 2001.

723 Pedrós-Alió, C., Calderón-Paz, J. I., Guixa-Boixereu, N., Estrada, M., Gasol, J. M.: Bacterioplankton

724 and phytoplankton biomass and production during summer stratification in the northwestern
725 Mediterranean Sea, *Deep-Sea Res. Pt. I*, 46, 985-1019, 1999.

726 Pérez, V., Fernández, E., Mara Ón, E., Morán, X., Zubkov, M. V.: Vertical distribution of
727 phytoplankton biomass, production and growth in the Atlantic subtropical gyres, *Deep-Sea Res. Pt. I*,
728 53, 1616-1634, 2006.

729 Pitarch, J., Odermatt, D., Kawka, M., Wüest, A.: Retrieval of vertical particle concentration profiles by
730 optical remote sensing: a model study, *Opt. Express*, 22, A947-A959, 2014.

731 Platt, T., Sathyendranath, S., Caverhill, C. M., Lewis, M. R.: Ocean primary production and available
732 light: further algorithms for remote sensing, *Deep-Sea Res. Pt. I*, 35, 855-879, 1988.

733 Prairie, J. C., Franks, P. J. S., Jaffe, J. S., Doubell, M. J., Yamazaki, H.: Physical and biological
734 controls of vertical gradients in phytoplankton, *Limnol. Oceanogr.*, 1, 75-90, 2011.

735 Raven, J. A., Richardson K.: Photosynthesis in marine environments. In: *Topics in Photosynthesis*,
736 Elsevier, Edited by N. R. Baker and Long S., 7, 337-399, 1986.

737 Richardson, A. J., Silulwane, N. F., Mitchell-Innes, B. A., Shillington, F. A.: A dynamic quantitative
738 approach for predicting the shape of phytoplankton profiles in the ocean, *Prog. Oceanogr.*, 59, 301-319,
739 2003.

740 Riley, G. A., Stommel, H., Bumpus, D. F.: Quantitative ecology of the plankton of the western North
741 Atlantic, *Bulletin Bingham Oceanogra. Collect.*, 12, 1-69, 1949.

742 Ryabov, A. B., Rudolf, L., Blasius, B.: Vertical distribution and composition of phytoplankton under
743 the influence of an upper mixed layer, *J. Theor. Biol.*, 263, 120-133, 2010.

744 Salihoglu, B., Garçon, V., Oschlies, A., Lomas, M. W.: Influence of nutrient utilization and
745 remineralization stoichiometry on phytoplankton species and carbon export: A modeling study at
746 BATS, *Deep-Sea Res. Pt. I*, 55, 73-107, 2008.

747 Sharples, J., Moore, C. M., Rippeth, T. P., Holligan, P. M., Hydes, D. J., Fisher, N. R., Simpson, J. H.:
748 Phytoplankton distribution and survival in the thermocline, *Limnol. Oceanogr.*, 46, 486-496, 2001.

749 Siswanto, E., Ishizaka, J., Yokouchi, K.: Estimating chlorophyll-a vertical profiles from satellite data
750 and the implication for primary production in the Kuroshio front of the East China Sea, *J. Oceanogr.*,
751 61, 575-589, 2005.

752 Sullivan, J. M., Donaghay, P. L., Rines, J. E.: Coastal thin layer dynamics: consequences to biology
753 and optics, *Cont. Shelf Res.*, 30, 50-65, 2010.

754 Sverdrup, H. U.: On conditions for the vernal blooming of phytoplankton, *J. Cons. int. Explor. Mer.*, 18,
755 287-295, 1953.

756 Takahashi, M., Hori, T.: Abundance of picophytoplankton in the subsurface chlorophyll maximum
757 layer in subtropical and tropical waters, *Mar. Biol.*, 79, 177-186, 1984.

758 Tjiputra, J. F., Polzin, D., Winguth, A. M.: Assimilation of seasonal chlorophyll and nutrient data into
759 an adjoint three - dimensional ocean carbon cycle model: Sensitivity analysis and ecosystem parameter
760 optimization, *Global Biogeochem. Cy.*, 21, GB1001, 1-13, 2007.

761 Varela, R. A., Cruzado, A., Tintoré, J.: A simulation analysis of various biological and physical factors
762 influencing the deep-chlorophyll maximum structure in oligotrophic areas, *J. Marine Syst.*, 5, 143-157,
763 1994.

764 Weston, K., Fernand, L., Mills, D. K., Delahunty, R., Brown, J.: Primary production in the deep
765 chlorophyll maximum of the central North Sea, *J. Plankton Res.*, 27, 909-922, 2005.

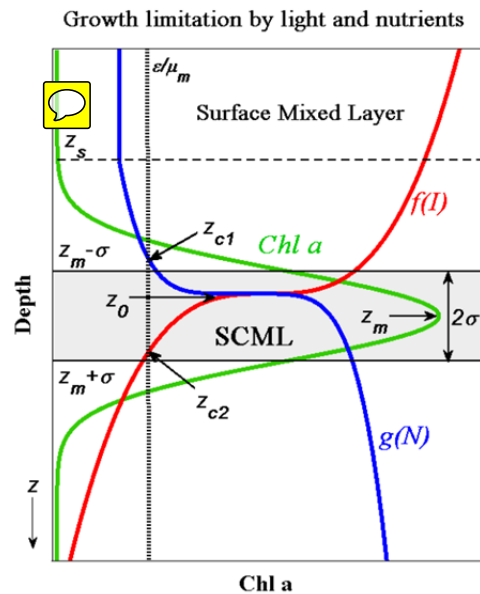
766 Williams, C., Sharples, J., Mahaffey, C., Rippeth, T.: Wind - driven nutrient pulses to the subsurface
767 chlorophyll maximum in seasonally stratified shelf seas, *Geophys. Res. Lett.*, 2013.

768 Wu Y. P., Gao K. S.: Photosynthetic response of surface water phytoplankton assemblages to different
769 wavebands of UV radiation in the South China Sea, *Acta Oceanol. Sin.*, 5, 146-151, 2011.

770 Yoshiyama, K., Mellard, J. P., Litchman, E., Klausmeier, C. A.: Phytoplankton competition for
771 nutrients and light in a stratified water column, *Am. Nat.*, 174, 190-203, 2009.

772 List of figures and tables

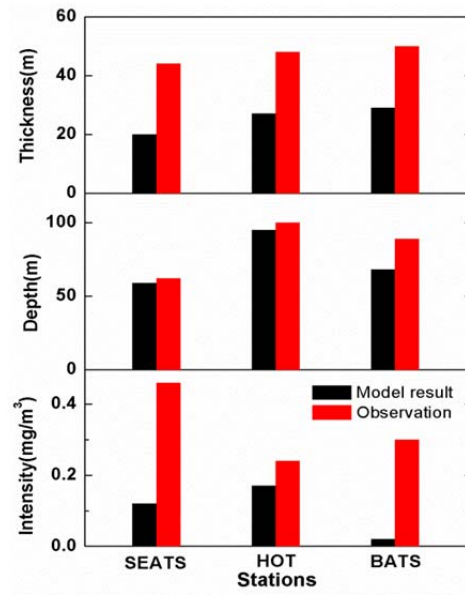
773 Figure 1



774

775 Fig. 1 Schematic picture of Chl a distribution under the limitation by light and nutrient in
776 stratified water column (red solid line is Chl a concentration as a function of depth; black dashed
777 line is the growth limiting term with respect to light, $f(I)$; blue dashed line is the growth limiting
778 term with respect to nutrients, $g(N)$; horizontal dashed line represents the depth of surface mixed
779 layer, z_s ; horizontal solid lines indicate the locations of the upper- and lower-SCML, $z_m - \sigma$, $z_m + \sigma$,
780 respectively; vertical dotted line is the ratio of loss rate to maximum growth rate, ε/μ_m ; z_{c1} and z_{c2}
781 refer to the two compensation depths where $\mu_m g(N) = \varepsilon$ and $\mu_m f(I) = \varepsilon$, respectively; z_0 and z_m
782 indicate the depths of maximum in growth rates and in Chl a concentrations, respectively; double
783 arrow represents the thickness of the SCML, 2σ)

784 Figure 2



785

786 Fig. 2 Comparisons of the model results and observations (in terms of thickness, depth, and
787 intensity of SCML) at SEATS, HOT, and BATS (black columns represent the model results, red
788 columns are the observations at the three stations which were fitted by Gaussian function using
789 annually averaged data obtained from <http://www.odn.ntu.edu.tw/>,
790 <http://hahana.soest.hawaii.edu/hot/hot-dogs/cextraction.html>, and <http://bats.bios.edu/>,
791 respectively)

792 Table 1 Influences of dynamic model parameters on the steady-state SCML thickness (2σ), depth
 793 (z_m), intensity (P_{max}), and the total Chl a in the water column (h).

Model parameters (\uparrow)	2σ	z_m	P_{max}	h
I_0 (Surface light intensity)	-	\uparrow	-	-
K_I (Half-saturation constant of light limited growth)	-	\downarrow	-	-
K_{v2} (Vertical diffusivity below surface mixed layer)	\uparrow	\downarrow	\uparrow	\uparrow
w (Sinking velocity of phytoplankton)	\downarrow	\downarrow	\uparrow	-
K_d (Light attenuation coefficient)	\downarrow	\downarrow	\uparrow	-
ε (Loss rate of phytoplankton)	\downarrow^*	\downarrow	/	\downarrow
	\uparrow^{**}	\downarrow	\downarrow	\downarrow
α (Nutrient recycling coefficient)	-	-	\uparrow	\uparrow
$\frac{dN}{dz} \Big _{z=z_b}$ Nutrient gradient at the lower boundary of SCML	-	-	\uparrow	\uparrow
K_N (Half-saturation constant of nutrient limited growth)	-	-	-	-
K_{v1} (Vertical diffusivity in surface mixed layer)	-	-	-	-
μ_{max} (Maximum growth rate of phytoplankton)	/	/	/	/

794 \uparrow indicates increase, \downarrow indicates decrease, - indicates no effect, / indicates no straightforward
 795 result, * indicates a result when $\varepsilon < \mu_{max}/2$, and ** indicates a result when $\varepsilon > \mu_{max}/2$.

796

Table 2 Parameter values at SEATS, HOT, and BATS

Parameters	Units	Values at Stations		
		SEATS	HOT	BATS
I_0	$\mu\text{mol photos m}^{-2} \text{s}^{-1}$	700 ^(1, 2)	550 ^(1, 3)	448 ^(1, 4)
K_d	m^{-1}	0.052 ^(1, 5)	0.04 ^(1, 3)	0.042 ^(1, 4)
K_{v2}	$\text{m}^2 \text{s}^{-1}$	$5 \cdot 10^{-5}$ ⁽⁶⁾	$5 \cdot 10^{-5}$ ⁽³⁾	$1 \cdot 10^{-4}$ ^(7, 8)
μ_{max}	d^{-1}	1.2 ^(9, 10)	0.96 ⁽³⁾	1 ⁽¹¹⁾
K_I	$\mu\text{mol photos m}^{-2} \text{s}^{-1}$	40 ⁽¹²⁾	20 ⁽³⁾	20 ^(3, 12, 13)
ε	d^{-1}	0.5 ^(9, 10)	0.24 ⁽³⁾	0.5 ⁽¹⁴⁾
α	-	0.3 ⁽¹⁰⁾	0.5 ⁽³⁾	0.16 ⁽⁸⁾
w	m d^{-1}	1 ⁽¹⁵⁾	1 ^(3, 15)	2 ⁽⁸⁾
dN/dz at depth of z_b	mmol N m^{-4}	0.1 ⁽¹⁶⁾	0.05 ^(17, 18)	0.02 ^(19, 20)
z_b	m	200	200	200

798 Superscripts refer to the references that provide the source for the parameter value and the
799 citations are as follows: ⁽¹⁾<http://oceandata.sci.gsfc.nasa.gov/SeaWiFS/Mapped/Annual/9km/>;
800 ⁽²⁾Wu and Gao, 2011; ⁽³⁾Huisman et al., 2006; ⁽⁴⁾Varela et al., 1994; ⁽⁵⁾Lee Chen et al., 2005; ⁽⁶⁾Lu
801 et al., 2010; ⁽⁷⁾Hood et al., 2001; ⁽⁸⁾Salihoglu et al., 2008; ⁽⁹⁾Cai et al., 2006; ⁽¹⁰⁾Liu et al., 2007;
802 ⁽¹¹⁾Ayata et al., 2013; ⁽¹²⁾Raven and Richardson, 1986; ⁽¹³⁾Mara On and Holligan, 1999;
803 ⁽¹⁴⁾Tjiputra et al., 2007; ⁽¹⁵⁾Bienfang and Harrison, 1984; ⁽¹⁶⁾Chen et al., 2006; ⁽¹⁷⁾Fennel and Boss,
804 2003; ⁽¹⁸⁾Beckmann and Hense, 2007; ⁽¹⁹⁾Cianca et al., 2007; ⁽²⁰⁾Cianca et al., 2012.